

## Review on hydrogen in silicon solar cells: From its origin to its detrimental effects

Benjamin Hammann <sup>a,b,\*</sup>, Florian Schindler <sup>b</sup>, Jonas Schön <sup>a,b</sup>, Wolfram Kwapił <sup>a,b</sup>, Martin C. Schubert <sup>b</sup>, Stefan W. Glunz <sup>a,b</sup>

<sup>a</sup> University of Freiburg, Department of Sustainable Systems Engineering (INATECH), Chair for Photovoltaic Energy Conversion, Emmy-Noether-Str. 2, 79110, Freiburg, Germany

<sup>b</sup> Fraunhofer Institute for Solar Energy ISE, Heidenhofstraße 2, 79110, Freiburg, Germany



### ARTICLE INFO

#### Keywords:

Hydrogen  
Silicon solar cells  
Degradation

### ABSTRACT

In this work, we present an overview of the current understanding of hydrogen in modern silicon solar cells. The ambivalent nature of hydrogen poses a significant challenge for solar cells: While hydrogen is highly beneficial due to the passivation of bulk and surface defects, it is also detrimental to long-term stability, being associated with two degradation phenomena. Specifically, we examine the relation between hydrogen and light- and elevated-temperature-induced degradation (LeTID) and surface-related degradation (SRD). Our findings indicate that LeTID is mitigated when total hydrogen concentrations are below  $5 \times 10^{14} \text{ cm}^{-3}$ . For the surface degradation of an aluminium oxide/silicon nitride ( $\text{Al}_2\text{O}_3/\text{SiN}_x:\text{H}$ ) passivation layer stack, our data indicate the existence of a similar upper tolerance limit. Thus, managing hydrogen content is key to reducing these degradation phenomena. Therefore, we discuss various strategies to control the hydrogen content. One important factor is the hydrogen source, typically hydrogen-rich silicon nitride. Furthermore, the hydrogen diffusion process is discussed that occurs mainly during the fast-firing step, including both in-diffusion at around the peak temperature and out-diffusion during subsequent cool-down. Additionally, we consider the effects of other interlayers, such as  $\text{Al}_2\text{O}_3$  or highly-doped surface-near layers, on the diffusion process. Thus, depending on the cell process, the most suitable adjustments can be employed to achieve optimum hydrogen management.

### 1. Introduction

Silicon-based solar cells play an important role in the global energy market. For c-Si photovoltaic modules that last over 30 years, it is essential to achieve both high power conversion efficiency and minimal degradation. For both aspects, hydrogen plays a key role. However, the impact of hydrogen is ambivalent. On one hand, hydrogen is known to passivate defects in the bulk and at the surface, e.g. Refs. [1–9], reducing recombination and thereby increasing efficiency. On the other hand, hydrogen is known to cause solar cells to degrade, being related to two degradation phenomena, e.g. Refs. [10–14].

This study discusses the state of knowledge on the relation of hydrogen with the two degradation phenomena, light- and elevated-temperature-induced degradation (LeTID), e.g. Refs. [15–17], and surface-related degradation (SRD), e.g. Refs. [18–20]. We review the correlation of the LeTID and SRD extent with the hydrogen content,

re-evaluate data from literature and describe the current model of how different hydrogen complexes and reactions interact and influence both degradation phenomena. We identify an optimal range of total hydrogen concentration, where no degradation extent is observed.

This balance can be achieved through specific technical adjustments in the manufacturing process, as for instance demonstrated in Ref. [21] for LeTID. To this end, we review the process of introducing hydrogen into silicon solar cells. This includes the impact of the hydrogen source, typically hydrogenated silicon nitride ( $\text{SiN}_x:\text{H}$ ), and the hydrogen diffusion during the fast-firing step. Furthermore, we discuss other important factors that can facilitate or hinder hydrogen diffusion. This results in a multifaceted view on controlling the hydrogen concentration to prevent hydrogen-related degradation.

\* Corresponding author: University of Freiburg, Department of Sustainable Systems Engineering (INATECH), Chair for Photovoltaic Energy Conversion, Emmy-Noether-Str. 2, 79110, Freiburg, Germany.

E-mail address: [benjamin.hammann@ise.fraunhofer.de](mailto:benjamin.hammann@ise.fraunhofer.de) (B. Hammann).

## 2. Experimental methods

Given that this work compares, reviews, and reassesses results from multiple studies, we provide only a brief overview of the various methods. For detailed information, readers are referred to the respective studies cited in the corresponding sections.

This study primarily focuses on *p*-type silicon, including results on boron-doped float-zone (FZ) and multicrystalline (mc) Si and on gallium-doped Czochralski (Cz) grown Si. Hydrogen content measurements vary across different studies. Some studies track resistivity changes during dark annealing to investigate changes in acceptor-hydrogen pairs [12,14,22–32]. Studying those changes through simulation [22,23,33–36] or with a subsequent illumination treatment [14, 30,32] allows the extraction of the total hydrogen concentration and the concentration of the main hydrogen complexes: molecular hydrogen and acceptor hydrogen pairs. Moreover, some studies employ low-temperature Fourier-transformed infrared (FT-IR) spectroscopy to directly measure the local vibrational modes of these complexes [12,13, 31,37,38], while other studies use secondary ion mass spectroscopy (SIMS) on deuterated samples [27,39].

Investigating hydrogen requires specially prepared sample structures. Often, degradation phenomena are investigated in parallel on the same samples by measuring changes in the effective lifetime of excess charge carriers through photoconductance decay (PCD) or photoluminescence (PL) measurements. Furthermore, PCD measurements allow the separation of bulk- and surface-related effects (compare, e.g., Refs. [40–42]), enabling a detailed study of defect kinetics and the estimation of formed defects.

## 3. Hydrogen and degradation

Hydrogen is known to be related to at least two degradation phenomena: light- and elevated-temperature-induced degradation (LeTID) and surface-related degradation (SRD). In this section, we discuss the main experimental findings on the relation between hydrogen and these degradation phenomena.

### 3.1. Light- and elevated-temperature-induced degradation (LeTID)

LeTID was first described in 2012 by Ramspeck et al. [15], and it broadly affects silicon solar cells independent of the wafer doping type (*n* or *p*-type, e.g. Refs. [43–45]), dopant element (B- or Ga-doped, e.g. Refs. [46,47]), or growth method (mc-, cast-mono, Cz, FZ-Si, e.g. Refs. [10,15,48,49]). Its connection to various manufacturing processes, such as deposited passivation layers, e.g. Refs. [50–53], or the fast-firing step, e.g. Refs. [54,55], has led to suggestions of a relationship between hydrogen and LeTID (compare, e.g., Ref. [10]). Schmidt et al. [11] were the first to observe a direct correlation, combining LeTID investigations on mc-Si with hydrogen investigations on FZ-Si. The corresponding data is shown in Fig. 1 (dark blue circles), depicting the increase of the LeTID extent with increasing total hydrogen concentration  $[H]_{\text{tot}}$ . Our similar investigations in B-doped FZ-Si material [36] are included as well (light blue diamonds). For Ga-doped material, Fig. 1 includes data from Zerfaß et al. [14] (dark green hexagons) and Simon et al. [32] (light green stars), re-evaluated to show the total hydrogen concentration by summing the contribution of the individual hydrogen complexes ( $2x[H_2] + [GaH] = [H]_{\text{tot}}$ ). Note the differences in maximum LeTID extent, which are likely due to varying treatment conditions and different excess charge carrier density  $\Delta n$  used to extract the LeTID extent. Additionally, the studies used different methods to determine  $[H]_{\text{tot}}$ , presumably resulting in further deviations.

Overall, a similar relationship between LeTID extent and  $[H]_{\text{tot}}$  is observed for both B-doped and Ga-doped samples. Furthermore, all studies reveal the same trend of the LeTID extent decreasing with  $[H]_{\text{tot}}$ . Our data and the data from Zerfaß et al. additionally show that zero LeTID extent is reached at around  $[H]_{\text{tot}} = 5 \times 10^{14} \text{ cm}^{-3}$ . This trend is

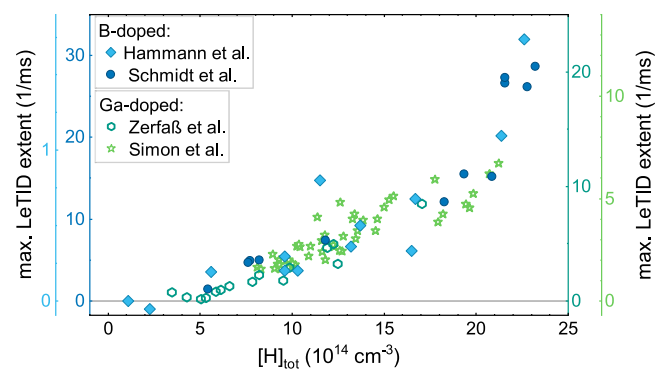


**Fig. 1.** Relation of the LeTID extent and the total hydrogen concentration for B-doped [11,36] (closed symbols) and Ga-doped samples [14] (open symbols). The Ga-doped data from Ref. [14] have been re-assessed in terms of  $[H]_{\text{tot}}$ . Note that the different studies use different treatment and evaluation conditions, not allowing a quantitative comparison of the LeTID extent between the studies. For a qualitative comparison, the data are scaled differently to be able to compare the observed trends.

evident not only in B-doped Si (as discussed in Ref. [36]), but also in Ga-doped Si. Thus, there is a range, where hydrogen is present, yet LeTID is suppressed. Therefore, we consider achieving hydrogen concentration below  $[H]_{\text{tot}} = 5 \times 10^{14} \text{ cm}^{-3}$  a key strategy to mitigate LeTID. In Section 4, we discuss various manufacturing methods to manipulate the hydrogen concentration to achieve such a low level. Note that, as detailed further below, the relevant complex for LeTID is molecular hydrogen,  $H_2$ , [12]. Therefore, the given limit serves as guidance, indicating that  $[H_2]$  is low enough such that no LeTID is observed. However, it is in principle possible to have lower  $[H]_{\text{tot}}$  than this limit, with enough  $[H_2]$  being available to still observe LeTID, as shown in the data from Zerfaß et al. [14] (two dark green data points in Fig. 1 with  $[H]_{\text{tot}} < 5 \times 10^{14} \text{ cm}^{-3}$  but max. LeTID extent  $> 0$ ).

### 3.2. Surface-related degradation (SRD)

During extended degradation investigations under LeTID conditions, a surface-related degradation (SRD) is often observed, which will be discussed in the following. Interestingly, some authors suggest a connection between SRD and LeTID, as SRD often occurs after LeTID regeneration, e.g. Refs. [19,56]. The degradation of surface passivation is observed for different passivation layers, although it is unclear whether they share the same underlying cause. For instance, Sperber et al. found that the degradation of a  $\text{SiN}_x:\text{H}$  layer is related to the chemical passivation [18], while for  $\text{Al}_2\text{O}_3/\text{SiN}_x:\text{H}$  stacks, it might involve both chemical passivation and fixed charge loss [57]. Furthermore, polysilicon-based passivation stacks featuring a thin tunneling oxide layer have also been shown to degrade under similar conditions, e.g. Refs. [58–60].

Because SRD is similarly affected by processing steps as LeTID, it is often suggested that SRD is also linked to hydrogen, e.g. Refs. [18–20, 56,58,61,62]. Compared to LeTID, fewer studies exist that investigate the connection between SRD and hydrogen. In dark annealing experiments, we observed that surface passivation degradation coincides with hydrogen presumably diffusing towards the surface, indicated by a decrease in BH pairs [12,36]. One of our studies, Ref. [13], provides the first experimental evidence for a correlation between the extent of SRD and hydrogen concentration. The corresponding data is depicted in Fig. 2, indicating larger surface degradation at higher hydrogen concentrations. Similar to LeTID, reducing hydrogen concentration  $[H]_{\text{tot}}$  mitigates surface passivation degradation. The trend suggests that an upper limit for  $[H]_{\text{tot}}$  might exist, with zero degradation extent below this limit. Although this data is based on  $\text{Al}_2\text{O}_3/\text{SiN}_x:\text{H}$  layers under dark annealing conditions, it is conceivable that other passivation stacks

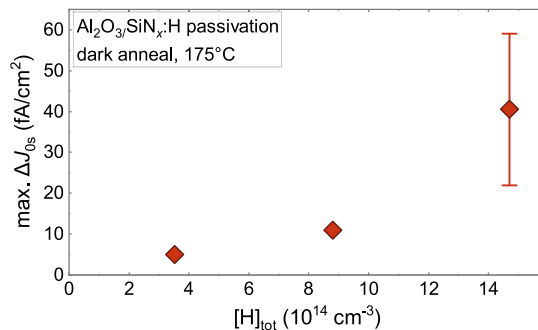


**Fig. 2.** Relation between the total hydrogen concentration  $[H]_{\text{tot}}$  and the surface degradation extent  $\Delta J_{0s}$ . To estimate the SRD extent, the difference in the surface recombination parameter  $J_{0s}$  between the degraded state and the initial value is calculated. The data is obtained on samples passivated with an  $\text{Al}_2\text{O}_3/\text{SiN}_x\text{H}$  layer stack, from Ref. [13]. Note that the uncertainty of the most degraded data point is due to different evaluation strategies, as detailed in Ref. [13].

exhibit a similar correlation. However, further research is necessary to investigate other stacks in more detail, which includes a potential upper limit of  $[H]_{\text{tot}}$  for SRD mitigation.

### 3.3. Interaction of hydrogen and defect states

While the total hydrogen concentration is an important figure for the severity of the degradation, the individual reactions governing these phenomena are linked to specific hydrogen complexes. In this section we provide an overview of the current state of knowledge, illustrated in Fig. 3. This figure outlines the various reactions and states for LeTID and SRD and what is currently known about hydrogen. Note that this is mainly valid for *p*-type Si. Three hydrogen complexes relevant to the degradation are shown: Molecular hydrogen ( $\text{H}_2$ ), acceptor-hydrogen (AH) pairs, and neutral/positively charged atomic hydrogen ( $\text{H}^{+0}$ ). Depending on the treatment conditions, different complexes are energetically favored. For instance, under dark annealing,  $\text{H}_2$  molecules dissociate to form AH pairs (compare, e.g., Ref. [35]). Under illumination, AH pairs dissociate, potentially resulting in the formation of  $\text{H}_2$ , e.g. Refs. [24,30,36]. Note, that in B-doped Si, BH pairs have also been observed to dissociate again during prolonged anneal. However, we presume that this is governed by the out-diffusion of hydrogen [36,63], not the formation of another hydrogen complex. Atomic hydrogen acts as an intermediate state in these reactions, with its charge state ratio dependent on temperature and excess charge carrier density [64].

The LeTID system was proposed to consist of four states [65]: The LeTID reservoir, precursor, defect, and the regenerated state. The degradation is known to be reversible under specific conditions, which is termed temporary recovery [66]. In Ref. [12], we identified  $\text{H}_2$  as the crucial complex influencing LeTID extent. Subsequent studies in Ga-doped material by Simon et al. and Zerfaß et al. confirmed similar

findings [14,32]. We attribute  $\text{H}_2$  to be part of the reservoir, reacting with an unknown complex, termed X, to form the LeTID precursor [36]. Our data, further detailed in Ref. [36], indicate the involvement of atomic hydrogen in the LeTID degradation and regeneration reaction.

For SRD, experiments indicate that hydrogen diffuses towards the surface during dark annealing [12] and illumination [30]. Monitoring the recombination rate showed an increase in surface-related recombination rate [12,30] in parallel to the dissociation of BH/GaH pairs. This suggests that surface passivation degradation is linked to hydrogen diffusion towards the surface. Our hypothesis is as follows: Upon reaching the surface/interface, hydrogen-related surface-near defects form, which are the cause for the observed degradation. Different possibilities for such defects exist, from hydrogen platelets, e.g. Ref. [67], to the de-passivation of H-passivated silicon dangling bonds by arriving atomic hydrogen, e.g. Ref. [68], or the creation of pinholes due to too high hydrogen concentrations [69,70]. However, the exact mechanism remains unclear, particularly with observations such as an increase in the interface defect density of some passivation layers but a decrease in the fixed charge density for other layers [18,57]. It is important to note the existence of a regeneration, e.g. Refs. [18,49], although experimental results are limited, particularly with regard to the influence of hydrogen.

### 4. Hydrogen management

Having discussed the importance of controlling the hydrogen concentration to mitigate degradation, we now demonstrate which parts of the solar cell manufacturing process can be adapted to manage hydrogen, as illustrated in Fig. 4. The introduction process involves two main factors: the source of hydrogen and its diffusion from the source throughout the sample. Typically, the source of hydrogen is a dielectric layer, with hydrogenated silicon nitride  $\text{SiN}_x\text{H}$  being the most common one.

During the fast-firing step, temperatures can reach 800 °C or more for a short duration, strongly increasing hydrogen diffusivity. This allows hydrogen to diffuse from its source throughout the solar cell.

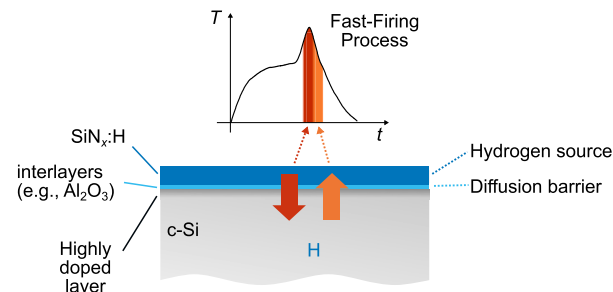


**Fig. 4.** Schematic overview of the main factors affecting the introduction of hydrogen into silicon solar cells. (For interpretation of the references to color in this figure legend, the reader is referred to the Web version of this article.)

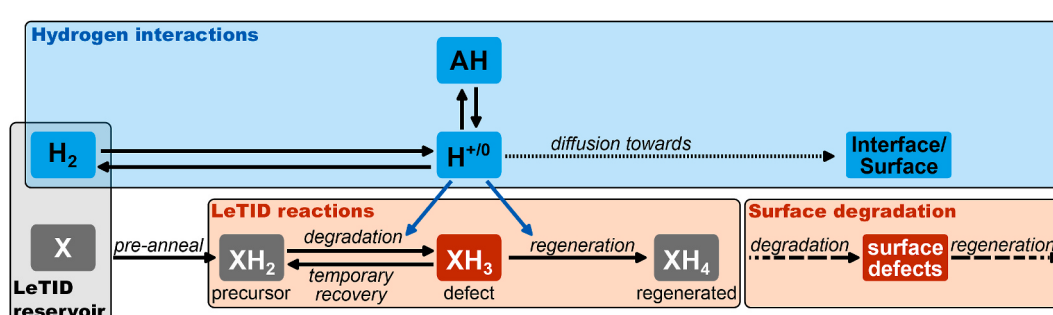


**Fig. 3.** Schematic overview of the interaction between hydrogen and the degradation phenomena, LeTID and SRD.

Notably, hydrogen is found to diffuse back out of the bulk during the subsequent cool-down. The diffusion process can be further influenced by diffusion barriers, such as an  $\text{Al}_2\text{O}_3$  interlayer, or highly doped layers. The following sections provide a detailed discussion of these influencing factors.

#### 4.1. The silicon nitride layer

Regarding the hydrogen source, we focus on the most common one: hydrogenated silicon nitride  $\text{SiN}_x:\text{H}$ . This layer is typically deposited using plasma-enhanced chemical vapor deposition (PECVD) tools, with deposition parameters significantly influencing the layer characteristics. A comprehensive study by Bredemeier et al. examined important layer parameters and their effect on the hydrogen concentration [23]. The main variation was the silane-to-ammonia ratio during deposition. The resulting change in layer characteristics is indicated with the refractive index,  $n$ , which shifts towards that of silicon ( $n = 3.9$ ) with increased silane content.

The total hydrogen concentration for silicon nitride layers deposited with varying silane-to-ammonia ratios from Ref. [23] is shown in Fig. 5 (light blue data). A characteristic behavior of an increase followed by a decrease in hydrogen concentration with rising refractive index is observed. According to Bredemeier et al. this behavior is closely related to the atomic density of the layer, which decreases as the refractive index increases. Initially, a lower layer density facilitates atomic hydrogen movement, leading to an increase in  $[\text{H}]_{\text{tot}}$ . Moreover, lower layer densities promote the formation of hydrogen molecules. However, the molecules are unable to enter the silicon, which is supposedly the cause for the observed  $[\text{H}]_{\text{tot}}$  decrease for larger refractive indices [23].

In [25], we have investigated similar samples, with different  $\text{SiH}_4/\text{NH}_3$  ratios, resulting in different  $\text{SiN}_x:\text{H}$  layer characteristics. The total hydrogen concentration data is shown in Fig. 5 (orange data). Our data from Ref. [25] exhibit a similar pattern of an increase followed by a decrease, suggesting the same physical mechanism presumably linked to the atomic density of the layer. Nonetheless, notable differences exist between the two studies. For instance, the maximum  $[\text{H}]_{\text{tot}}$  occurs at different refractive indices ( $n = 2.4$  vs  $n = 2.19$ ). Additionally, we could not detect any hydrogen concentration at  $n = 2.5$ , whereas Bredemeier's data show only a slight decrease. We attribute these differences to tool-to-tool variations, resulting in different layer characteristics despite identical refractive index. In Ref. [23], a laboratory-type PECVD tool from Oxford instruments is used, while an industrial inline PECVD tool from Roth&Rau is used in Ref. [25]. We presume that the main

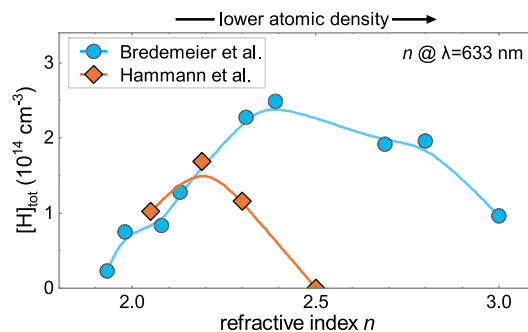


**Fig. 5.** Total hydrogen concentration after fast-firing for samples with different  $\text{SiH}_4/\text{NH}_3$  ratios during the  $\text{SiN}_x:\text{H}$  deposition, resulting in different refractive indices  $n$ . Data are from two separate studies (Bredemeier et al. [23], Hammann et al. [25]), with the data point at  $n = 2.5$  from the study by Hammann et al. being published in this work for the first time. Note that different hydrogen models are used to calculate  $[\text{H}]_{\text{tot}}$ , making a quantitative comparison between the two studies difficult. Lines are b-splines, serving as guide-to-the-eyes.  $[\text{H}]_{\text{tot}}$  is obtained from tracking resistivity during dark annealing, refractive index  $n$  at 633 nm is obtained with ellipsometry measurements.

difference is the static vs. dynamic deposition process, though other process parameters, such as temperature, might also play a role. Therefore, no universal trend of  $[\text{H}]_{\text{tot}}$  with the refractive index can be inferred. Instead, it is advisable to investigate tool-specific characteristics when aiming to maximize or minimize hydrogen concentration through  $\text{SiN}_x:\text{H}$  layer adaption.

#### 4.2. The fast-firing step

The investigations discussed in the previous section include a fast-firing step after the  $\text{SiN}_x:\text{H}$  deposition, since the fast-firing process is necessary for hydrogen to diffuse from the silicon nitride layer throughout the wafer. For such investigations, consistency in the fast-firing step is crucial, as even minor deviations in process parameters can significantly affect the hydrogen concentration. The reason for that is discussed in this section, alongside the important parameters and their respective effect.

##### 4.2.1. The impact of the peak temperature

The peak temperature of the fast-firing step is one key parameter determining the in-diffused hydrogen content. Fig. 6 presents experimental data for  $[\text{H}]_{\text{tot}}$  in samples fired with different peak temperatures,  $T_{\text{peak}}$ , from studies by Helmich et al. and Winter et al. [26,34]. The studies also examined variations in  $\text{SiN}_x:\text{H}$  layer characteristics, denoted by the different refractive indices,  $n$ .

Each data set shows an exponential relationship between  $[\text{H}]_{\text{tot}}$  and  $T_{\text{peak}}$ , as illustrated by the linear fits on the semilogarithmic graph (dashed lines). This implies that even small changes in  $T_{\text{peak}}$  can significantly alter the hydrogen concentration. We want to further highlight the influence of the  $\text{SiN}_x:\text{H}$  layer. As shown in Fig. 6, the temperature dependence varies for different  $\text{SiN}_x:\text{H}$  layer characteristics. For instance, Helmich's samples with  $n = 1.9$  exhibit a much lower increase in  $[\text{H}]_{\text{tot}}$  with  $T_{\text{peak}}$  compared to the other two parameters. In comparison, all samples from Winter et al. show a stronger increase, again indicating tool-to-tool differences, with the  $n = 2.1$  samples showing the lowest slope.

Note that to obtain  $[\text{H}]_{\text{tot}}$ , the data from Winter et al. [26] are re-evaluated for this study using the improved hydrogen model from Ref. [35], while the data from Helmich et al. are taken directly from their contribution [34], which used a different hydrogen model [71]. Therefore, a direct comparison of hydrogen concentrations between the two studies does not make sense.

We want to highlight a result by Chen et al. [17] showing that the LeTID extent also increases exponentially with the peak firing temperature. This is in accordance with the relation between hydrogen and

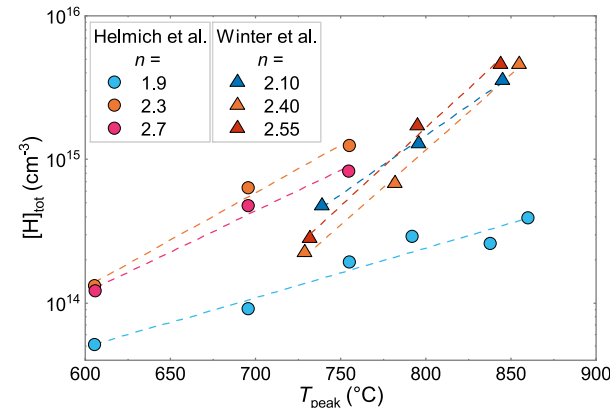


**Fig. 6.** Total hydrogen concentration after the fast-firing process for samples fired with different peak temperatures  $T_{\text{peak}}$  and different refractive indices  $n$  from two studies, Helmich et al. [34] and Winter et al. [26]. Dashed lines are linear fits to demonstrate the exponential relation between  $[\text{H}]_{\text{tot}}$  and  $T_{\text{peak}}$ .

$T_{\text{peak}}$  in Fig. 6, which is another demonstration for the link between hydrogen and LeTID, showing the importance of the peak temperature for mitigating LeTID.

#### 4.2.2. The impact of the cooling ramp

During the fast-firing step, the temperature rapidly increases until it reaches the peak. Around this peak, hydrogen diffuses from its source into the silicon bulk. During the subsequent cool-down hydrogen can diffuse back out of the silicon bulk. This out-diffusion was already presumed in studies like Refs. [55,72,73], and later experimentally demonstrated in Refs. [12,13]. Based on our experimental results in Ref. [13], we developed a model in Sentaurus TCAD [74] that describes the in- and out-diffusion of hydrogen. The key advancement is assuming a segregation process for hydrogen at the silicon surface (compare [63]). The segregation coefficient is temperature-dependent, resulting in an in-diffusion of hydrogen at peak temperatures that quickly switches to a pronounced out-diffusion when the sample cools down. In the model, the silicon nitride acts as a near-infinite source (sink) for hydrogen diffusing into (out of) the silicon bulk, with the process being limited by the hydrogen diffusion within the silicon bulk. Note that no direct experimental data of hydrogen at the  $\text{SiN}_x/\text{Si}$  interface is available. Therefore, it is also conceivable that hydrogen congregates at the interface or in a region close to the interface.

Experimentally, the hydrogen out-diffusion during the cool-down is investigated in Ref. [13] by maintaining the temperature at a specific value for 5.5 s. Two temperature plateaus are chosen: 560 and 660 °C, with a peak temperature of 800 °C. The experimental data in Fig. 7 show that less hydrogen is present in the samples with a temperature plateau compared to the reference sample without a plateau (plateau temperature = 25 °C).

The simulation in Fig. 7 models the same firing process while varying the temperature of the plateau, demonstrating good accordance with the experimental data. Our results indicate that the out-diffusion of hydrogen is particularly pronounced between 600 and 700 °C. Therefore, introducing large hydrogen concentrations with a high peak temperature can be counteracted by slowing down the cooling ramp in this critical temperature range. Finally, it is important to note that the sample thickness also impacts the in- and out-diffusion [12,63].

#### 4.3. The impact of interlayers

In addition to the above-described processes and layers, silicon solar

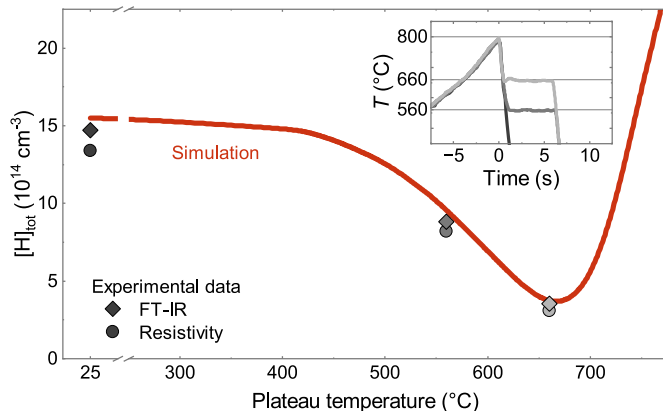


**Fig. 7.** Total depth-averaged hydrogen concentration after different firing steps which include a plateau during the cooling ramp. Experimental data are based on a 5.5 s plateau at defined temperatures of 560 and 660 °C (compare inset, light grey and grey colors) and without a plateau (dark grey colors). The simulation, discussed in more detail in Ref. [63] replicates the same 5.5 s plateau while varying the temperature, with the experimental data originally published in Ref. [13]. (For interpretation of the references to color in this figure legend, the reader is referred to the Web version of this article.)

cells typically feature further layers and processes, resulting in complex structures. For instance,  $\text{SiN}_x:\text{H}$  is typically used as an anti-reflective capping layer, while other layers, such as aluminium oxide,  $\text{Al}_2\text{O}_3$ , or silicon oxide,  $\text{SiO}_2$ , are used for passivating the silicon surface. Furthermore, highly-doped in-diffused layers or deposited and doped polycrystalline/amorphous Si layers are used to enhance charge carrier selectivity. In principle, all of these layers can influence the diffusion of hydrogen, although the impact on hydrogen diffusion has only been experimentally investigated for a few.

Focusing on layers that have been investigated, Fig. 8 shows the impact of  $\text{Al}_2\text{O}_3$  on hydrogen diffusion, with data from Helmich et al. [34] and Schmid et al. [27]. In both studies, hydrogen (or deuterium in Schmid's study) diffuses from the  $\text{SiN}_x:\text{H}(\text{D})$  layer through the  $\text{Al}_2\text{O}_3$  layer. Both studies observe that the measured hydrogen (deuterium) concentration decreases with thicker  $\text{Al}_2\text{O}_3$  layers, demonstrating that  $\text{Al}_2\text{O}_3$  acts as a diffusion barrier for hydrogen (deuterium).

Note that  $\text{Al}_2\text{O}_3$  can also act as a hydrogen source, for instance, for hydrogen passivation of tunnel-oxide passivating contacts (TOPCon) [8].  $\text{Al}_2\text{O}_3$  also being a hydrogen source might explain why the measured hydrogen content does not reach zero but instead saturates. Note that the exact barrier functionality is not yet clear.

Regarding highly doped, in-diffused layers near the surface, Fischer et al. used resistivity and SIMS measurements to investigate the diffusion properties [39]. They found that such a layer does not impede diffusion but might even increase hydrogen diffusion. In a different study using FT-IR spectroscopy, Aßmann et al. found nearly identical hydrogen concentration in samples with and without highly doped layers [38]. Therefore, it is most likely that such highly doped layers do not hinder the in-diffusion of hydrogen, but there is still some uncertainty regarding the hypothesis that these layers facilitate the hydrogen diffusion.

## 5. Conclusion

This work discusses the importance of controlling hydrogen for silicon solar cells. We review the connection between hydrogen and two degradation phenomena: Light- and elevated-temperature-induced degradation (LeTID) and surface-related degradation (SRD). For both phenomena, we find that their extent increases with the total

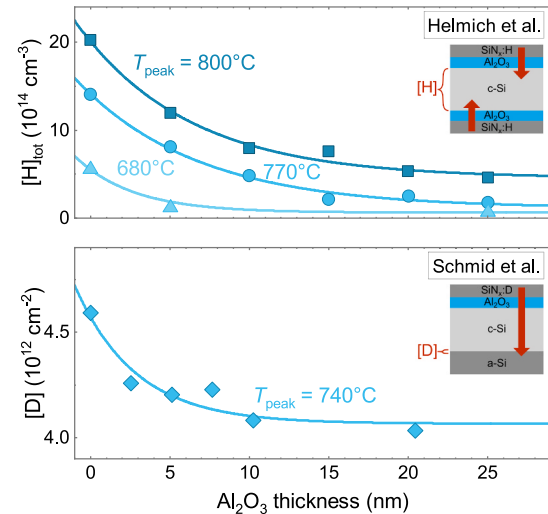


**Fig. 8.** Experimental data showing the impact of  $\text{Al}_2\text{O}_3$  as a diffusion barrier. Different methods are used to investigate the diffused hydrogen: a) the hydrogen concentration in the Si bulk is measured with resistivity measurements [34], b) the deuterium concentration at the a-Si/Si interface is measured with SIMS, after the deuterium is diffused through the  $\text{Al}_2\text{O}_3$  layer and the Si bulk (compare schematic insets). Lines are exponential fits serving as guide-to-the-eye.

concentration of hydrogen. Therefore, we discuss various factors influencing the introduction of hydrogen. By understanding the influence of different process parameters, it is possible to manipulate the hydrogen content to mitigate both degradation phenomena. Key factors include the composition of the hydrogen source, hydrogenated silicon nitride, the peak temperature and cooling rate of the fast-firing step, and interlayers such as  $\text{Al}_2\text{O}_3$ .

The challenge of controlling hydrogen varies across different solar cell technologies. While LeTID is the main degradation phenomenon for p-type passivated emitter and rear contact (PERC) solar cells, e.g. Ref. [75], (besides BO degradation, e.g. Ref. [76]), SRD becomes more significant for next-generation solar cells such as tunnel-oxide passivating contacts (TOPCon) solar cells, e.g. Ref. [77]. With different layer structures including highly-doped poly-Si layers, it is important to have sufficient hydrogen available for excellent surface passivation, e.g. Refs. [8,70], while avoiding degradation, e.g. Ref. [58]. Thus, careful control of hydrogen is and will be crucial.

### CRediT authorship contribution statement

**Benjamin Hammann:** Writing – review & editing, Writing – original draft, Visualization, Investigation, Formal analysis, Data curation, Conceptualization. **Florian Schindler:** Writing – review & editing, Supervision, Project administration, Funding acquisition, Conceptualization. **Jonas Schön:** Writing – review & editing, Software, Investigation. **Wolfram Kwapił:** Writing – review & editing, Supervision, Project administration, Funding acquisition. **Martin C. Schubert:** Writing – review & editing, Supervision, Project administration, Funding acquisition. **Stefan W. Glunz:** Writing – review & editing, Supervision, Project administration.

### Declaration of generative AI and AI-assisted technologies in the writing process

During the preparation of this work the authors used ChatGPT 4o in order to assess the grammar, spelling and readability. After using this tool, the authors reviewed and edited the content as needed and take full responsibility for the content of the published article.

### Declaration of competing interest

The authors declare that they have no known competing financial interests or personal relationships that could have appeared to influence the work reported in this paper.

### Acknowledgement

This work was supported by the German Federal Ministry for Economic Affairs and Climate Action (Contract no. 03EE1052B and 03EE1052D). Benjamin Hammann wants to thank the Stiftung Nagelschneider for funding his dissertation project.

### Data availability

Data will be made available on request.

### References

- [1] S.J. Pearton, J.W. Corbett, T.S. Shi, Hydrogen in crystalline semiconductors, *Appl. Phys. A* 43 (3) (1987) 153–195, <https://doi.org/10.1007/BF00615975>.
- [2] R. Lüdemann, Hydrogen passivation of multicrystalline silicon solar cells, *Mater. Sci. Eng., B* 58 (1–2) (1999) 86–90, [https://doi.org/10.1016/S0921-5107\(98\)00288-8](https://doi.org/10.1016/S0921-5107(98)00288-8).
- [3] A.G. Aberle, Surface passivation of crystalline silicon solar cells: a review, *Prog. Photovoltaics Res. Appl.* 8 (5) (2000) 473–487, [https://doi.org/10.1002/1099-159X\(200009/10\)8:5<473::AID-PIP337>3.0.CO;2-D](https://doi.org/10.1002/1099-159X(200009/10)8:5<473::AID-PIP337>3.0.CO;2-D).
- [4] S. Wilking, A. Herguth, G. Hahn, Influence of hydrogen on the regeneration of boron-oxygen related defects in crystalline silicon, *J. Appl. Phys.* 113 (19) (2013) 194503, <https://doi.org/10.1063/1.4804310>.
- [5] B. Hallam, C. Chan, M. Abbott, S. Wenham, Hydrogen passivation of defect-rich n-type Czochralski silicon and oxygen precipitates, *Sol. Energy Mater. Sol. Cells* 141 (2015) 125–131, <https://doi.org/10.1016/j.solmat.2015.05.009>.
- [6] C. Sun, A. Liu, S.P. Phang, F.E. Rougieux, D. Macdonald, Charge states of the reactants in the hydrogen passivation of interstitial iron in P-type crystalline silicon, *J. Appl. Phys.* 118 (8) (2015) 85709, <https://doi.org/10.1063/1.4929757>.
- [7] B.J. Hallam, P.G. Hamer, A.M. Ciesla née Wenham, C.E. Chan, B. Vicari Stefani, S. Wenham, Development of advanced hydrogenation processes for silicon solar cells via an improved understanding of the behaviour of hydrogen in silicon, *Prog. Photovoltaics Res. Appl.* 96 (1) (2020) 173, <https://doi.org/10.1002/pip.3240>.
- [8] J.-I. Polzin, B. Hammann, T. Niewelt, W. Kwapił, M. Hermle, F. Feldmann, Thermal activation of hydrogen for defect passivation in poly-Si based passivating contacts, *Sol. Energy Mater. Sol. Cells* 230 (2021) 111267, <https://doi.org/10.1016/j.solmat.2021.111267>.
- [9] J.A.T. de Guzman, V.P. Markevich, D. Hiller, I.D. Hawkins, M.P. Halsall, A. R. Peaker, Passivation of thermally-induced defects with hydrogen in float-zone silicon, *J. Phys. D Appl. Phys.* 54 (27) (2021) 275105, <https://doi.org/10.1088/1361-6463/ab8070>.
- [10] T. Niewelt, F. Schindler, W. Kwapił, R. Eberle, J. Schön, M.C. Schubert, Understanding the light-induced degradation at elevated temperatures: similarities between multicrystalline and floatzone p-type silicon, *Prog. Photovoltaics Res. Appl.* 26 (8) (2017) 533–542, <https://doi.org/10.1002/pip.2954>.
- [11] J. Schmidt, D. Bredemeier, D.C. Walter, On the defect physics behind light and elevated temperature-induced degradation (LeTID) of multicrystalline silicon solar cells, *IEEE J. Photovoltaics* 9 (6) (2019) 1497–1503, <https://doi.org/10.1109/JPHOTOV.2019.2937223>.
- [12] B. Hammann, N. Assmann, P.M. Weiser, W. Kwapił, T. Niewelt, F. Schindler, R. Sondena, E.V. Monakhov, M.C. Schubert, The impact of different hydrogen configurations on light- and elevated-temperature-induced degradation, *IEEE J. Photovoltaics* 13 (2) (2023) 224–235, <https://doi.org/10.1109/JPHOTOV.2023.3236185>.
- [13] B. Hammann, N. Aßmann, J. Schön, W. Kwapił, F. Schindler, S. Roder, E. V. Monakhov, M.C. Schubert, Understanding the impact of the cooling ramp of the fast-firing process on light- and elevated-temperature-induced degradation, *Sol. Energy Mater. Sol. Cells* 259 (2023) 112462, <https://doi.org/10.1016/j.solmat.2023.112462>.
- [14] R. Zerfaß, J. Simon, A. Herguth, G. Hahn, Impact of hydrogen in Ga-doped silicon on maximum LeTID defect density, *Sol. RRL* 7 (22) (2023) 2300501, <https://doi.org/10.1002/solr.202300501>.
- [15] K. Ramspeck, S. Zimmermann, H. Nagel, A. Metz, Y. Gassenbauer, B. Birkmann, A. Seidl, Light induced degradation of rear passivated mc-Si solar cells, 27th Eur. Photovolt. Sol. Energy Conf. Exhib. 1 (2012) 861, <https://doi.org/10.4229/27THEUPSEC2012-2DO.3.4>.
- [16] F. Kersten, P. Engelhart, H.-C. Ploigt, A. Stekolnikov, T. Lindner, F. Stenzel, M. Bartzsch, A. Szpeth, K. Petter, J. Heitmann, J.W. Müller, Degradation of multicrystalline silicon solar cells and modules after illumination at elevated temperature, *Sol. Energy Mater. Sol. Cells* 142 (2015) 83–86, <https://doi.org/10.1016/j.solmat.2015.06.015>.
- [17] D. Chen, M. Vaqueiro Contreras, A. Ciesla, P. Hamer, B. Hallam, M. Abbott, C. Chan, Progress in the understanding of light- and elevated-temperature-induced degradation in silicon solar cells: a review, *Prog. Photovoltaics Res. Appl.* 29 (11) (2020) 1180–1201, <https://doi.org/10.1002/pip.3362>.
- [18] D. Sperber, A. Graf, D. Skorka, A. Herguth, G. Hahn, Degradation of surface passivation on crystalline silicon and its impact on light-induced degradation experiments, *IEEE J. Photovoltaics* 7 (6) (2017) 1627–1634, <https://doi.org/10.1109/Jphotov.2017.2755072>.
- [19] K. Kim, R. Chen, D. Chen, P. Hamer, A. Ciesla née Wenham, S. Wenham, Z. Hameiri, Degradation of surface passivation and bulk in p-type monocrystalline silicon wafers at elevated temperature, *IEEE J. Photovoltaics* 9 (1) (2019) 97–105, <https://doi.org/10.1109/JPHOTOV.2018.2878971>.
- [20] P. Hamer, D. Chen, R.S. Bonilla, Thermal processes and their impact on surface-related degradation, *Phys. Status Solidi RRL* (2021) 2100464, <https://doi.org/10.1002/psrr.202100464>.
- [21] F. Maischner, W. Kwapił, J.M. Greulich, Y. Jung, H. Höffler, P. Saint-Cast, M. C. Schubert, S. Rein, S.W. Glunz, Process influences on LeTID in Ga-doped silicon, *Sol. Energy Mater. Sol. Cells* 260 (2023) 112451, <https://doi.org/10.1016/j.solmat.2023.112451>.
- [22] D.C. Walter, D. Bredemeier, R. Falster, V.V. Voronkov, J. Schmidt, Easy-to-apply methodology to measure the hydrogen concentration in boron-doped crystalline silicon, *Sol. Energy Mater. Sol. Cells* 200 (2019) 109970, <https://doi.org/10.1016/j.solmat.2019.109970>.
- [23] D. Bredemeier, D.C. Walter, R. Heller, J. Schmidt, Impact of silicon nitride film properties on hydrogen in-diffusion into crystalline silicon, 36th Eur. Photovolt. Sol. Energy Conf. Exhib. 1 (2019) 112–115, <https://doi.org/10.4229/EUPVSEC20192019-2AO.4.4>.
- [24] D.C. Walter, D. Bredemeier, R. Falster, J. Schmidt, V.V. Voronkov, Disappearance of hydrogen-boron-pairs in silicon during illumination and its relevance to lifetime degradation and regeneration effects in solar cells, 37th Eur. Photovolt. Sol. Energy Conf. Exhib. 1 (2020) 140–144, <https://doi.org/10.4229/EUPVSEC20202020-2AO.5.1>.
- [25] B. Hammann, L. Rachdi, W. Kwapił, F. Schindler, M.C. Schubert, Insights into the hydrogen-related mechanism behind defect formation during light- and elevated-

- temperature-induced degradation, *Phys. Status Solidi RRL* 15 (6) (2021) 2000584, <https://doi.org/10.1002/pssr.202000584>.
- [26] C. Winter, J. Simon, A. Herguth, Study on boron–hydrogen pairs in bare and passivated float-zone silicon wafers, *Phys. Status Solidi A* 218 (23) (2021) 2100220, <https://doi.org/10.1002/pssa.202100220>.
- [27] A. Schmid, C. Fischer, D. Skorka, A. Herguth, C. Winter, A. Zuschlag, G. Hahn, On the role of AlOx thickness in AlOx/SiNy:H layer stacks regarding light- and elevated temperature-induced degradation and hydrogen diffusion in c-Si, *IEEE J. Photovoltaics* 11 (4) (2021) 967–973, <https://doi.org/10.1109/JPHOTOV.2021.3075850>.
- [28] D.C. Walter, V.V. Voronkov, R. Falster, D. Bredemeier, J. Schmidt, On the kinetics of the exchange of hydrogen between hydrogen–boron pairs and hydrogen dimers in crystalline silicon, *J. Appl. Phys.* 131 (16) (2022) 165702, <https://doi.org/10.1063/5.0086307>.
- [29] Y. Acker, J. Simon, A. Herguth, Formation dynamics of BH and GaH-pairs in crystalline silicon during dark annealing, *Phys. Status Solidi A* 219 (17) (2022) 2200142, <https://doi.org/10.1002/pssa.202200142>.
- [30] J. Simon, A. Herguth, L. Kutschera, G. Hahn, The dissociation of gallium–hydrogen pairs in crystalline silicon during illuminated annealing, *Phys. Status Solidi RRL* (2022) 2200297, <https://doi.org/10.1002/pssr.202200297>.
- [31] R. Søndenå, P.M. Weiser, E. Monakhov, Direct and indirect determination of hydrogen–boron complexes in float-zone silicon wafers, in: *SiliconPV 2021*, the 11th International Conference on Crystalline Silicon Photovoltaics, Hamelin, Germany/Online, 2022 130012, <https://doi.org/10.1063/5.0089274>.
- [32] J. Simon, R. Fischer-Stüblin, R. Zerfaß, L. Kutschera, P. Dufke, A. Herguth, S. Roder, G. Hahn, Correlation study between LeTID defect density, hydrogen and firing profile in Ga-doped crystalline silicon, *Sol. Energy Mater. Sol. Cells* 260 (2023) 112456, <https://doi.org/10.1016/j.solmat.2023.112456>.
- [33] D. Bredemeier, D.C. Walter, R. Heller, J. Schmidt, Impact of hydrogen-rich silicon nitride material properties on light-induced lifetime degradation in multicrystalline silicon, *Phys. Status Solidi RRL* 13 (8) (2019) 1900201, <https://doi.org/10.1002/pssr.201900201>.
- [34] L. Helmich, D.C. Walter, D. Bredemeier, J. Schmidt, Atomic-layer-deposited Al2O3 as effective barrier against the diffusion of hydrogen from SiNx:H layers into crystalline silicon during rapid thermal annealing, *Phys. Status Solidi RRL* (2020) 2000367, <https://doi.org/10.1002/pssr.202000367>.
- [35] P. Vieira Rodrigues, B. Hammann, N. Abmann, J. Schön, W. Kwapił, T. Niewelt, F. Schindler, E.V. Monakhov, M.C. Schubert, Doping dependence of boron–hydrogen dynamics in crystalline silicon, *J. Appl. Phys.* 136 (8) (2024) 085703, <https://doi.org/10.1063/5.0215089>.
- [36] B. Hammann, P. Vieira Rodrigues, N. Abmann, W. Kwapił, F. Schindler, M. C. Schubert, S.W. Glunz, Deciphering the role of hydrogen in the degradation of silicon solar cells under light and elevated temperature, *Sol. RRL* 8 (20) (2024) 2400457, <https://doi.org/10.1002/solr.202400457>.
- [37] P.M. Weiser, E. Monakhov, H. Haug, M.S. Wiig, R. Søndenå, Hydrogen-related defects measured by infrared spectroscopy in multicrystalline silicon wafers throughout an illuminated annealing process, *J. Appl. Phys.* 127 (6) (2020) 65703, <https://doi.org/10.1063/1.5142476>.
- [38] N. Abmann, R. Søndenå, B. Hammann, W. Kwapił, E. Monakhov, Reducing time and costs of FT-IR studies of the effect of SiNx, dopants, and emitter on hydrogen species in Si wafers and solar cell structures, *SiliconPV Conf Proc* 1 (2023), <https://doi.org/10.52825/siliconpv.v1.840>.
- [39] C. Fischer, A. Schmid, A. Herguth, A. Zuschlag, P.P. Altermatt, P. Hamer, G. Hahn, Influence of highly doped layers on hydrogen in-diffusion into crystalline silicon, *Sol. Energy Mater. Sol. Cells* 250 (2023) 112056, <https://doi.org/10.1016/j.solmat.2022.112056>.
- [40] A. Herguth, On the lifetime-equivalent defect density: properties, application, and pitfalls, *IEEE J. Photovoltaics* 9 (5) (2019) 1182–1194, <https://doi.org/10.1109/JPHOTOV.2019.2922470>.
- [41] B. Hammann, B. Steinhauser, A. Fell, R. Post, T. Niewelt, W. Kwapił, A. Wolf, A. Richter, H. Höffler, M.C. Schubert, Quantifying surface recombination — improvements in determination and simulation of the surface recombination parameter  $J_{0S}$ , *IEEE J. Photovoltaics* 13 (4) (2023) 535–546, <https://doi.org/10.1109/JPHOTOV.2023.3265859>.
- [42] A. Herguth, J. Kamphues, On the impact of bulk lifetime on the quantification of recombination at the surface of semiconductors, *IEEE J. Photovoltaics* (2023) 1–10, <https://doi.org/10.1109/JPHOTOV.2023.3291453>.
- [43] H.C. Sio, H. Wang, Q. Wang, C. Sun, W. Chen, H. Jin, D. Macdonald, Light and elevated temperature induced degradation in p-type and n-type cast-grown multicrystalline and mono-like silicon, *Sol. Energy Mater. Sol. Cells* 182 (2018) 98–104, <https://doi.org/10.1016/j.solmat.2018.03.002>.
- [44] D. Chen, P.G. Hamer, M. Kim, T.H. Fung, G. Bourret-Sicotte, S. Liu, C.E. Chan, A. Ciesla, R. Chen, M.D. Abbott, B.J. Hallam, S.R. Wenham, Hydrogen induced degradation: a possible mechanism for light- and elevated temperature- induced degradation in n-type silicon, *Sol. Energy Mater. Sol. Cells* 185 (2018) 174–182, <https://doi.org/10.1016/j.solmat.2018.05.034>.
- [45] C. Vargas, S. Nie, D. Chen, C. Chan, B. Hallam, G. Coletti, Z. Hameiri, Degradation and recovery of n -type multi-crystalline silicon under illuminated and dark annealing conditions at moderate temperatures, *IEEE J. Photovoltaics* 9 (2) (2019) 355–363, <https://doi.org/10.1109/JPHOTOV.2018.2885711>.
- [46] W. Kwapił, J. Dalke, R. Post, T. Niewelt, Influence of dopant elements on degradation phenomena in B- and Ga-doped czochralski-grown silicon, *Sol. RRL* 5 (5) (2021) 2100147, <https://doi.org/10.1002/solr.202100147>.
- [47] J.M. Fritz, A. Zuschlag, D. Skorka, A. Schmid, G. Hahn, Temperature dependent degradation and regeneration of differently doped mc-Si materials, *Energy Proc.* 124 (2017) 718–725, <https://doi.org/10.1016/j.egypro.2017.09.085>.
- [48] D. Chen, M. Kim, B.V. Stefani, B.J. Hallam, M.D. Abbott, C.E. Chan, R. Chen, D. N. Payne, N. Nampalli, A. Ciesla, T.H. Fung, K. Kim, S.R. Wenham, Evidence of an identical firing-activated carrier-induced defect in monocrystalline and multicrystalline silicon, *Sol. Energy Mater. Sol. Cells* 172 (2017) 293–300, <https://doi.org/10.1016/j.solmat.2017.08.003>.
- [49] D. Sperber, A. Heilemann, A. Herguth, G. Hahn, Temperature and light-induced changes in bulk and passivation quality of boron-doped float-zone silicon coated with SiNx:H, *IEEE J. Photovoltaics* 7 (2) (2017) 463–470, <https://doi.org/10.1109/jphotov.2017.2649601>.
- [50] F. Kersten, J. Heitmann, J.W. Müller, Influence of Al2O3 and SiNx passivation layers on LeTID, *Energy Proc.* 92 (2016) 828–832, <https://doi.org/10.1016/j.egypro.2016.07.079>.
- [51] U. Varshney, M. Abbott, A. Ciesla, D. Chen, S. Liu, C. Sen, M. Kim, S. Wenham, B. Hoex, C. Chan, Evaluating the impact of SiNx thickness on lifetime degradation in silicon, *IEEE J. Photovoltaics* 9 (3) (2019) 601–607, <https://doi.org/10.1109/Jphotov.2019.2896671>.
- [52] J. Lindroos, A. Zuschlag, D. Skorka, G. Hahn, Silicon nitride deposition: impact on lifetime and light-induced degradation at elevated temperature in multicrystalline silicon, *IEEE J. Photovoltaics* 10 (1) (2020) 8–18, <https://doi.org/10.1109/JPHOTOV.2019.2945164>.
- [53] U. Varshney, M. Kim, M.U. Khan, P. Hamer, C. Chan, M. Abbott, B. Hoex, Impact of substrate thickness on the degradation in multicrystalline silicon, *IEEE J. Photovoltaics* 11 (1) (2021) 65–72, <https://doi.org/10.1109/JPHOTOV.2020.3038412>.
- [54] C.E. Chan, D.N.R. Payne, B.J. Hallam, M.D. Abbott, T.H. Fung, A.M. Wenham, B. S. Tjahjono, S.R. Wenham, Rapid stabilization of high-performance multicrystalline P-type silicon PERC cells, *IEEE J. Photovoltaics* 6 (6) (2016) 1473–1479, <https://doi.org/10.1109/JPHOTOV.2016.2606704>.
- [55] R. Eberle, W. Kwapił, F. Schindler, M.C. Schubert, S.W. Glunz, Impact of the firing temperature profile on light induced degradation of multicrystalline silicon, *Phys. Status Solidi RRL* 10 (12) (2016) 861–865, <https://doi.org/10.1002/pssr.201600272>.
- [56] D. Chen, P. Hamer, M. Kim, C. Chan, A. Ciesla nee Wenham, F. Rougieux, Y. Zhang, M. Abbott, B. Hallam, Hydrogen-induced degradation: explaining the mechanism behind light- and elevated temperature-induced degradation in n- and p-type silicon, *Sol. Energy Mater. Sol. Cells* 207 (2020) 110353, <https://doi.org/10.1016/j.solmat.2019.110353>.
- [57] D. Sperber, A. Schwarz, A. Herguth, G. Hahn, Enhanced stability of passivation quality on diffused silicon surfaces under light-induced degradation conditions, *Sol. Energy Mater. Sol. Cells* 188 (2018) 112–118, <https://doi.org/10.1016/j.solmat.2018.08.019>.
- [58] Di Kang, H.C. Sio, Di Yan, W. Chen, J. Yang, J. Jin, X. Zhang, D. Macdonald, Long-term stability study of the passivation quality of polysilicon-based passivation layers for silicon solar cells, *Sol. Energy Mater. Sol. Cells* 215 (2020) 110691, <https://doi.org/10.1016/j.solmat.2020.110691>.
- [59] M. Winter, S. Bordihn, R. Peibst, R. Brendel, J. Schmidt, Degradation and regeneration of n+-doped poly-Si surface passivation on p-type and n-type Cz-Si under illumination and dark annealing, *IEEE J. Photovoltaics* 10 (2) (2020) 423–430, <https://doi.org/10.1109/JPHOTOV.2020.2964987>.
- [60] D. Chen, C. Madumelu, M. Kim, B.V. Stefani, A. Soeriyadi, Di Kang, H.C. Sio, X. Zhang, P. Zhu, B. Hallam, M. Wright, Investigating the degradation behaviours of n+-doped Poly-Si passivation layers: an outlook on long-term stability and accelerated recovery, *Sol. Energy Mater. Sol. Cells* 236 (2022) 111491, <https://doi.org/10.1016/j.solmat.2021.111491>.
- [61] B. Hammann, J. Engelhardt, D. Sperber, A. Herguth, G. Hahn, Influencing light and elevated temperature induced degradation and surface-related degradation kinetics in float-zone silicon by varying the initial sample state, *IEEE J. Photovoltaics* 10 (1) (2020) 85–93, <https://doi.org/10.1109/JPHOTOV.2019.2954768>.
- [62] C. Madumelu, Y. Cai, C. Hollemani, R. Peibst, B. Hoex, B.J. Hallam, A. H. Soeriyadi, Assessing the stability of p+ and n+ polysilicon passivating contacts with various capping layers on p-type wafers, *Sol. Energy Mater. Sol. Cells* 253 (2023) 112245, <https://doi.org/10.1016/j.solmat.2023.112245>.
- [63] J. Schön, P. Hamer, B. Hammann, C. Zechner, W. Kwapił, M.C. Schubert, Hydrogen in silicon solar cells: the role of diffusion, *Sol. RRL* 9 (1) (2025) 2400668, <https://doi.org/10.1002/solr.202400668>.
- [64] C. Sun, F.E. Rougieux, D. Macdonald, A unified approach to modelling the charge state of monatomic hydrogen and other defects in crystalline silicon, *J. Appl. Phys.* 117 (4) (2015) 45702, <https://doi.org/10.1063/1.4906465>.
- [65] T.H. Fung, M. Kim, D. Chen, C.E. Chan, B.J. Hallam, R. Chen, D.N. Payne, A. Ciesla, S.R. Wenham, M.D. Abbott, A four-state kinetic model for the carrier-induced degradation in multicrystalline silicon: introducing the reservoir state, *Sol. Energy Mater. Sol. Cells* 184 (2018) 48–56, <https://doi.org/10.1016/j.solmat.2018.04.024>.
- [66] W. Kwapił, J. Schön, T. Niewelt, M.C. Schubert, Temporary recovery of the defect responsible for light- and elevated temperature-induced degradation: insights into the physical mechanisms behind LeTID, *IEEE J. Photovoltaics* 10 (6) (2020) 1591–1603, <https://doi.org/10.1109/JPHOTOV.2020.3025240>.
- [67] N.M. Johnson, F.A. Ponce, R.A. Street, R.J. Nemanich, Defects in single-crystal silicon induced by hydrogenation, *Phys. Rev. B* 35 (8) (1987) 4166–4169, <https://doi.org/10.1103/physrevb.35.4166>.
- [68] E. Cartier, J.H. Stathis, D.A. Buchanan, Passivation and depassivation of silicon dangling bonds at the Si/SiO<sub>2</sub> interface by atomic hydrogen, *Appl. Phys. Lett.* 63 (11) (1993) 1510–1512, <https://doi.org/10.1063/1.110758>.
- [69] A. Diggs, Z. Crawford, A. Goga, Z. Zhao, J. Stuckelberger, G.T. Zimányi, Pinhole Formation by nucleation-driven phase separation in TOPCon and POLO solar cells:

- structural dynamics and optimization, *ACS Appl. Energy Mater.* 7 (8) (2024) 3414–3423, <https://doi.org/10.1021/acsaem.4c00171>.
- [70] Di Kang, H. C. Sio, J. Stuckelberger, R. Liu, Di Yan, X. Zhang, D. Macdonald, "Optimum hydrogen injection in phosphorus-doped polysilicon passivating contacts," *ACS Appl. Mater. Interfaces*, early access. doi: 10.1021/acsami.1c17342.
- [71] V.V. Voronkov, R. Falster, Formation, dissociation, and diffusion of various hydrogen dimers in silicon, *Phys. Status Solidi B* 254 (6) (2017) 1600779, <https://doi.org/10.1002/pssb.201600779>.
- [72] S. Wilking, S. Ebert, A. Herguth, G. Hahn, Influence of hydrogen effusion from hydrogenated silicon nitride layers on the regeneration of boron-oxygen related defects in crystalline silicon, *J. Appl. Phys.* 114 (19) (2013) 194512, <https://doi.org/10.1063/1.4833243>.
- [73] F. Maischner, S. Maus, J. Greulich, S. Lohmüller, E. Lohmüller, P. Saint-Cast, D. Ourinson, H. Vahlman, K. Hergert, S. Riepe, S. Glunz, S. Rein, LeTID mitigation via an adapted firing process in p-type PERC cells from SMART cast-
- monocrystalline, Czochralski and high-performance multicrystalline silicon, *Prog. Photovoltaics Res. Appl.* 30 (2) (2021) 3467, <https://doi.org/10.1002/pip.3467>.
- [74] Synopsis, Sentaurus TCAD: Release Q-2019.12. [Online]. Available: [www.synopsys.com](http://www.synopsys.com).
- [75] M.A. Green, The passivated emitter and rear cell (PERC): from conception to mass production, *Sol. Energy Mater. Sol. Cells* 143 (2015) 190–197, <https://doi.org/10.1016/j.solmat.2015.06.055>.
- [76] T. Niewelt, J. Schön, W. Warta, S.W. Glunz, M.C. Schubert, Degradation of crystalline silicon due to boron–oxygen defects, *IEEE J. Photovoltaics* 7 (1) (2017) 383–398, <https://doi.org/10.1109/Jphotov.2016.2614119>.
- [77] S.W. Glunz, B. Steinhauser, J.-I. Polzin, C. Luderer, B. Grübel, T. Niewelt, A.M.O. M. Okasha, M. Bories, H. Nagel, K. Krieg, F. Feldmann, A. Richter, M. Bivour, M. Hermle, Silicon-based passivating contacts: the TOPCon route, *Prog. Photovoltaics Res. Appl.* (2021) 3522, <https://doi.org/10.1002/pip.3522>.